

FLOODABLE CROSS-SECTIONAL AREA AND SLOPE TO THE NEAREST DRAINAGE AS EXTENSIONS OF THE HAND MODEL: MAPPING FLOOD SUSCEPTIBILITY IN THE REGION OF LUCAS DO RIO VERDE, MATO GROSSO STATE, BRAZIL

ÁREAS DA SEÇÃO TRANSVERSAL INUNDÁVEL E DECLIVIDADE EM RELAÇÃO AO CURSO D'ÁGUA MAIS PRÓXIMO COMO EXTENSÕES DO MODELO HAND: MAPEAMENTO DE SUSCEPTIBILIDADE À INUNDAÇÃO NA REGIÃO DE LUCAS DO RIO VERDE, MATO GROSSO, BRASIL

ÁREAS DE SECCIÓN TRANSVERSAL INUNDABLE Y DECLIVIDAD EN RELACIÓN AL CURSO DE AGUA MÁS CERCANO COMO EXTENSIÓN AL MODELO HAND: MAPEO DE SUSCEPTIBILIDAD A INUNDACIÓN EN LA REGIÓN DE LUCAS DO RIO VERDE, MATO GROSSO, BRASIL

Vitor Vieira Vasconcelos

Universidade Federal do ABC, Centro de Engenharia, Modelagem e Ciências Sociais Aplicadas, São Bernardo do Campo, Brasil.

vitor.v.v@gmail.com

Ciro Lótfi Vaz

WayCarbon, Universidade Federal do Rio de Janeiro, Brasil

[ciroh@gmail.com](mailto:cirobh@gmail.com)

Marco Follador

WayCarbon, Instituto BioAtlântica, Itália

mfollador@waycarbon.com

Melina Amoni Silveira Alves

WayCarbon, Pontifícia Universidade Católica de Minas Gerais, Belo Horizonte, Brasil

melina.amoni@waycarbon.com

ABSTRACT

The HAND (Height Above the Nearest Drainage) model has been applied as a robust indicator for mapping flood susceptibility and the gradients of hydrological-edaphic-ecological processes. This paper extends the HAND model by combining the vertical and horizontal distances in relation to the nearest drainage to generate the indicators of floodable cross-sectional area and slope to the nearest drainage. The HAND, cross-sectional area, conventional slope, and slope to the nearest drainage indicators are combined for distinct analyses of flood susceptibility mapping in the Lucas do Rio Verde region, Mato Grosso State, Brazil. The indicators of cross-sectional area and slope to the nearest drainage were spatially consistent with the expected hydrogeomorphological characteristics. The maps based on floodable cross-sectional area, when compared to those based on the HAND model, were more restrictive in areas further from watercourses, especially when combined with slope classes.

Keywords: Flood; GIS; HAND; Rio Verde; Spatial analysis; Water resources.

RESUMO

O modelo HAND (*Height Above the Nearest Drainage*) tem sido aplicado como um indicador robusto para mapeamento de susceptibilidade a inundações e gradientes de processos hidrológicos-edáficos-ecológicos. Este artigo estende o modelo HAND ao combinar a altura e a distância horizontal em relação ao corpo hídrico mais próximo, para gerar indicadores da área da seção transversal inundável e

a declividade em relação ao corpo hídrico mais próximo. Os indicadores HAND, área da seção transversal, declividade convencional e declividade em relação ao corpo hídrico mais próximo são combinadas de forma a testar diferentes possibilidades de mapeamento de susceptibilidade a inundações, com aplicação na região do Lucas do Rio Verde, em Mato Grosso, Brasil. Os indicadores de área de seção transversal e de declividade em relação a corpo hídrico mais próximo apresentaram-se espacialmente consistentes com as características hidrogeomorfológicas esperados. Os mapas utilizando a área da seção transversal alagável, se comparados ao HAND, foram mais restritivos em áreas mais distantes aos cursos de água, especialmente quando combinados com as classes de declividade.

Palavras-chave: Inundação; SIG; HAND; Rio Verde; Análise espacial; Recursos hídricos.

RESUMEN

El modelo HAND (*Height Above the Nearest Drainage*) ha sido aplicado como un indicador robusto para mapeo de susceptibilidad a inundaciones e gradientes de procesos hidrológicos-edáficos-ecológicos. Este artículo extiende el modelo HAND combinando la altura y la distancia horizontal em relación al cuerpo hídrico más cercano, para generar indicadores del área de sección transversal inundable e la declividad en relación a el cuerpo hídrico más cercano. Los indicadores HAND, área de la sección transversal, declividad convencional y declividad en relación al cuerpo hídrico más cercano fueron combinados para probar diferentes posibilidades de mapeo de susceptibilidad a inundaciones, con una aplicación en la región de Lucas do Rio Verde, en Mato Grosso, Brasil. Los indicadores de área de sección transversal y de declividad en relación al cuerpo hídrico más cercano se presentan espacialmente consistentes con las características hidrogeomorfológicas esperadas. Los mapas utilizando el área de la sección transversal inundable, si se comparan con el HAND, fueron más restrictivos en áreas más distantes a los cursos de agua, especialmente cuando se combinan con las clases de declividad.

Palabras clave: Inundación; SIG; HAND; Rio Verde; Análisis espacial; Recursos hídricos.

INTRODUCTION

The Height Above the Nearest Drainage (HAND) model is based on a digital elevation model (DEM), and the drainage network is used as a relative reference. An initial height of 0 meters is established, and the heights to the remaining cells of the DEM are recalculated following the overland flow routes to the nearest water body (RENNÓ et al., 2008; NOBRE et al., 2011). In this method, the height is not defined by altimetry but in relation to the terrain unevenness to the nearest stream. The resulting indicator is helpful for estimating the water table depth, soil humidity and flood propensity based on a DEM and hydrographic data (NOBRE et al., 2011a; SILVA et al., 2011). Therefore, in the literature, HAND has been referred to either as a model (when focusing on flow route modeling) or an indicator (when focusing on the final output value per raster pixel). As a territorial planning tool, the height to the nearest drainage is useful for flood susceptibility estimation, wetland delineation based on geotechnical restrictions for building, and the conservation of the environmental and hydrological services of wetlands (VARALLO et al., 2016).

After the HAND model was proposed by Rennó et al. (2008), many Geographical Information Systems (GISs) have incorporated algorithms to measure this indicator (Table 1). However, before the use of the HAND model, Rennó et al. (2008) noted that DEMs should be pre-processed through entrenching (burning) depressions rather than simply filling them because entrenchment better preserves the hydrologic flow routes of the original DEM. The best algorithms in Table 1 calculate the HAND indicator using the original DEM and a flow route model from a pre-processed and hydrologically consistent second DEM. In this approach, the HAND model is not affected by changes in the DEM cells during the pre-processing phase. Additionally, Table 1 shows whether each algorithm complementarily generates the horizontal distance to the nearest stream, in addition to HAND (i.e., the vertical distance), using the same flow route to the nearest drainage as a reference.

Table 1: A comparison of the algorithms used to generate the HAND model

Software	HAND using a hydrologically consistent DEM	HAND using an original DEM (and hydrologically consistent flow routes)	Horizontal distance to the nearest drainage
ArcGIS	Yes	Yes (Taudem)	Yes
QGIS	Yes (Taudem, WOIS script in R)	Yes (Taudem)	Yes (Taudem)
SAGA	Yes	No	Yes
GRASS	Yes	Yes	Yes
Terraview (TerraHidro)	Yes	Yes	No
Taudem	Yes	Yes	Yes
Whitebox GAT	Yes	Yes	Yes
ANA HAND App	Yes	Yes	No
INPE HAND App	Yes	Yes	No

Source: the authors.

Based on an analysis of many recent papers that employed the HAND model (Table 2), a relative robustness in the classes of the HAND indicator was observed based on the attributes of the hydrological dynamics and the distinct characteristics of the study area. However, these studies noted that local variabilities must be considered, and the method must be adjusted accordingly, such as in the case of the human disruption of a drainage network or

in distinct hydrogeomorphological contexts (floodplains, headwaters, etc.) (DIAS, 2014; NOBRE et al., 2015).

In addition to the HAND approach, another research method presented in the academic literature attempts to map flood susceptibility based on the slope, horizontal distance to rivers and altimetry stratification. Table 3 presents some of these studies and the respective slope classes. Although the slope classes are relatively consistent, these studies emphasize that the horizontal distance and altimetry stratification vary significantly according to the environmental characteristics of each mapped area (DED, 2013; PRINA; TRETIN, 2014; CHAVES; PEIXOTO FILHO, 2015). This finding is in agreement with the findings of Silva et al. (2012), who proposed that the height to the nearest drainage is a more robust criterion for delimiting ecologically and hydrologically relevant areas than is using only the horizontal distance in the method currently stipulated by Brazilian environmental laws.

This paper proposes the use of the floodable cross-sectional area and slope to the nearest drainage as extensions of the HAND model. In this context, the HAND indicator, conventional slope, slope to the nearest drainage, and floodable cross-sectional area are applied and tested in the region of Lucas do Rio Verde to evaluate their spatial results regarding flood susceptibility. The study area is within the Rio Verde Basin, in the state of Mato Grosso and was selected due to the interest of food chain companies in evaluating the flood risks of their units in this area.

Table 2: Classifications of HAND indicators in the academic literature

Study Area	HAND Classes	Characteristics	References
Amazon, Asu, Brazil	0-5.3 - Floodplain 5.3 -15 - Ecotone > 15 - High land (changes to plateaus for slopes < 7.5%)	Forested environment of high land systems (flooded seasonally), equatorial climate	Rennó et al. (2008); Nobre et al. (2011b)
São Paulo city, including the Tietê and Pinheiros Rivers, Brazil	The same as Rennó et al. (2008)	Hill, terrace and plain systems, tropical climate	Nobre et al. (2011a)
Wark Catchment, Grand Duchy of Luxembourg	0-5.9 - Wetland ecosystems > 5.9 - High land (changes to plateaus for slopes < 0.129)	82 km ² basin, temperate climate	Gharari (2011a; 2011b; 2014)
Manaus Municipality, Brazil	The same as Rennó et al. (2008)	Confluence of the Negro and Solimões Rivers in the Amazon River basin, equatorial climate	Rodrigues et al. (2011)
Confluence of the Negro and Solimões, Brazil	< 8 - Floodable areas > 8 - Non-floodable areas	Floodplain of large basins, equatorial climate	Alfaya (2012)
Grijalva-Usumacinta catchment, southeastern Mexican states of Tabasco and Chiapas	< 8 - Floodable > 8 - Not floodable Validated with remote sensing classification	Tropical climate	Schlaffer et al. (2012)
Paraíba do Sul River Basin, Brazil	≤ 5 - Lowlands, flooded or floodable areas 6 to 15 - Transitional areas and ecotones	Mountainous relief with entrenched valleys, tropical climate	Silva et al. (2013)

FLOODABLE CROSS-SECTIONAL AREA AND SLOPE TO THE NEAREST DRAINAGE AS EXTENSIONS OF
THE HAND MODEL: MAPPING FLOOD SUSCEPTIBILITY IN THE REGION OF LUCAS DO RIO VERDE,
MATO GROSSO STATE, BRAZIL

Study Area	HAND Classes	Characteristics	References
	16 to 50 - Slopes > 50 - Hills Validated with a hydraulic model in which the floodable area was 80% lowlands and 20% ecotones.		
Ouro Preto city, Brazil	< 5.15 - Floodable areas	Mountainous relief with entrenched valleys, tropical mountainous climate	Santos et al. (2013)
Chao Phraya River Basin, Thailand	0-1 - Area with high flood susceptibility	Flood plain of a large basin	Westerhoff et al. (2013)
Rio Grande do Sul State, Brazil	The HAND limit in flooded areas of paddy varied from 8 to 40 meters depending on the area. The majority of the flooded area was below 5.5 meters in the HAND model.	Plain to gently wavy relief, temperate climate	Mengue (2013)
Upper Heihe River, China	< 5 - Wet ecosystem > 5 m with slope <0.1 - Terrace > 5 m with slope >0.1 - Hillslope	Mountainous relief, cold temperate climate	Gao et al. (2014)
Mid-basin of the Araguaia River, Brazil	Different flood limits, depending on the altimetry in the basin: Altimetry..... HAND > 260 m < 2 240-260 m < 3 220-180 m < 5	Seasonal floodplain with murundu fields, equatorial climate	Dias (2014)
Nile basin in Sudan and Chad	< 6 - Floodable areas Validated with remote sensing	Plains and humid downstream, and desert with an alluvial plain upstream	Guzinski et al. (2014)
Lower Magdalena River basin, Colômbia	HAND.....Return period < 2.8.....2.33 years < 5.5.....20 years < 7.8..... 100 years	Flood plain, equatorial climate	Mesa (2014)
Confluence of the Severn and Avon Rivers, southwestern United Kingdom	< 10 - Floodable > 10 - Not floodable Validated with remote sensing	Temperate climate	Schlaffer et al. (2015)
Itajaí-Açú River Valley, Brazil	< 13 - Maximum flood level in 2011	Flood plain, temperate climate	Nobre (2015)

Source: the authors.

Table 3: Values for slope classification for flood susceptibility evaluation in the academic literature

Study area	Classification	Characteristics of the study area	Reference
Theoretical work (no specific study area)	< 2% - Well-defined floodplain if the river is not entrenched	Theoretical work	Rosgen (1994)
Theoretical work (no specific study area)	< 2% - Plain areas that become floodable if they are near the drainage network 2-5% - Plain areas characterized by sediment depositional processes 5-15% - Wavy areas with moderate surface dynamics leading to accentuated erosive processes > 15% - Hillslopes vulnerable to landslides and mass movements	Theoretical work with classes based on the experience of the Technological Research Institute (IPT) of São Paulo State	Moreira and Pires Neto (1998)
High Itu River basin, in the municipalities of Santiago, Unistalda and São Francisco de Assis in the state of Rio Grande do Sul, Brazil	The same as Moreira and Pires Neto (1998)	Temperate climate, headwaters of the basin	Trentin and Robaina (2005)

Study area	Classification	Characteristics of the study area	Reference
Right bank floodplain of the Mooki River between the cities of Caroonna and Breeza, South Wales State, Australia	< 2%, as defined by the Water Act of 1912	Floodplain surrounded by ridges, arid to semi-arid climate	NSW (2006)
St. Lucia Island and a detailed flood map of the City of Castries	< 1% - Floodplains and high flood susceptibility areas 1-5% - Medium flood susceptibility > 5% - Low flood susceptibility These areas were selected using maps of land cover type, soil type and rainfall intensity.	Island, tropical climate	Cooper and Opadeyi (2006)
Czech Moravian geomorphological region	< 2% - Well-defined floodplains 2-4% - Small, narrow pockets of floodplains can occur > 4% - No development of floodplains These values were determined based on slope combined with the height and distance to the nearest river.	Floodplain and alluvial plain of large river basins, temperate continental climate	Ded (2013)
Municipality of Alegre in Espírito Santo State, Brazil	Slope Flood susceptibility 0-2% Very high 2-5% High 5-10% Medium 10-15% Low > 15% Very low Combined with flood height levels	Tropical climate	Temporim et al. (2013)
Município de Jaguari, Rio Grande do Sul State, Brazil	The same as Moreira and Pires Neto (1998) combined with altimetry data	Municipality with frequent flood events, temperate climate	Prina and Tretin (2014)
Administrative Region of Fercal in Distrito Federal, Brazil	The same as Moreira and Pires Neto (1998) combined with altimetry data and calibrated with field observations	Municipality with frequent flood events, mountainous temperate climate	Chaves and Peixoto Filho (2015)

Source: the authors.

MATERIAL AND METHODS

Study Area

The study region is within the Rio Verde Basin, which comprises parts of the municipalities of Lucas do Rio Verde, Sorriso and Tapurah in Mato Grosso State, Brazil (Figure 1). The Rio Verde Basin is a tributary of the Paranaíba River Basin, which drains to the Paraná Basin. The region is characterized by gentle and wavy relief. Additionally, the basin is in a transition region between a mountainous tropical climate and a humid equatorial climate, with an average rainfall of 1,722.1 mm concentrated between September and April (LUBITZ et al., 2011). The flow of the Rio Verde in Lucas do Rio Verde is greater than or equal to 66.1 m³/s 95% of the time, greater than or equal to 83.2 m³/s 75% of the time, and greater than 225 m³/s 3% of the time (LUBTIZ et al., 2011). The area was originally a

transition region from Brazilian Savana (Cerrado) to Amazon Forest; however, the area is currently dominated by extensive mechanized and irrigated agriculture, except for some remaining strips of riparian vegetation.



Figure 1: Location of the study area

Source: the authors.

Methods

The primary basis for the analyses was a Shuttle Radar Topography Mission (SRTM) DEM of the region of Lucas do Rio Verde (JARVIS, et al., 2008) with a resolution of 90 m. The spatial and statistical algorithms used the entire SRTM scene (enclosed by a red polygon in Figure 1). However, due to scale issues, the results for only the black dashed polygon of Figure 1 are presented in this paper, in order to assist with visual interpretation.

The DEM was pre-processed for hydrological consistency using a drainage entrenchment method with a threshold depth of 8 meters (half of the standard deviation error of the SRTM DEM). This process was performed in SAGA 2.1.2 software using the “Sink Removal” algorithm. Then, the remaining depressions were filled with the “Depressionless Map” algorithm in Grass 7 software. In Grass 7, the “r.watershed” algorithm was used to

generate the flow routes over the hydrologically consistent DEM with threshold parameters of 150 m² for the minimum basin area without drainage and 150 meters for the minimum linear flow without drainage. Then, using the “r.stream.distance” algorithm in Grass 7, the HAND indicator values (vertical distance to the nearest river and horizontal distance to the nearest river) were generated using the altimetry reference of the original DEM (before pre-processing) and the flow routes generated by the “r.watershed” algorithm from the hydrologically consistent DEM.

In the SAGA environment, the original DEM was used to calculate the slope (in percent) using a second-order polynomial algorithm with 8 parameters (ZEVENBERGEN; THORNE, 1987). The floodable cross-sectional area and the slope to the nearest drainage, both based on the vertical and horizontal distance to a drainage, were calculated using map algebra, as illustrated in Figures 2 and 3. The underlying goal of using the floodable cross-sectional area is to estimate how much the cross-sectional area of a river would need to increase to flood a specific pixel in the terrain. Both approaches (floodable cross-sectional area and slope to the nearest drainage) are based on two-dimensional relief instead of using only one dimension, which has been commonly employed in HAND model studies.

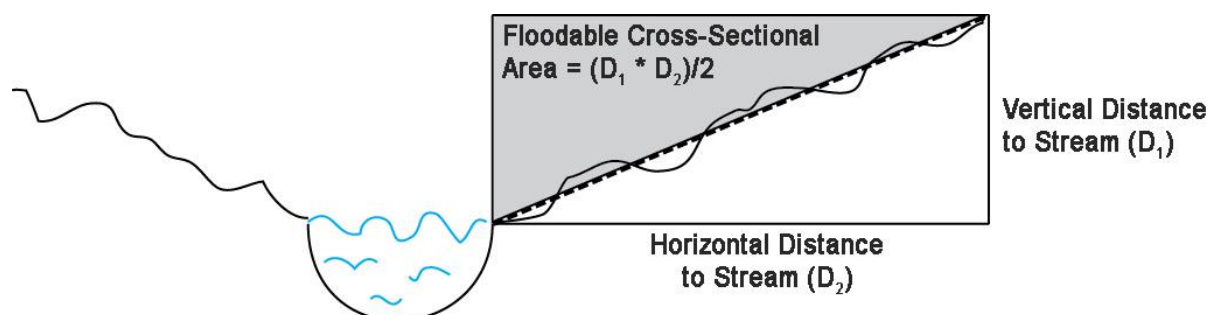


Figure 2: Illustration of the method used to calculate the floodable cross-sectional area
Source: the authors.

Based on the classification limits of the HAND and slope indicators in the academic literature (Tables 2 and 3), Table 4 and 5 provide the proposed classifications of HAND and slope values, respectively. Based on the combined classification of the slope and an auxiliary indicator proposed by Pina and Tretin (2014) and Chavez and Peixoto (2015) and using the classification values presented in Tables 4 and 5, Table 6 was generated by combining HAND and slope indices to evaluate flood susceptibility. In this paper, the slope classes of Tables 5 and 6 were applied both to the conventional slope and to the slope to the nearest drainage.

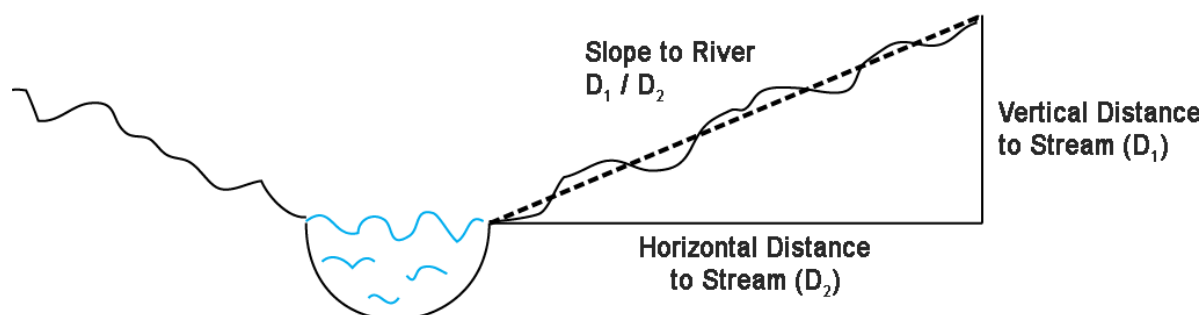


Figure 3: Illustration of the method used to calculate the slope to the nearest drainage
Source: the authors.

Table 4: Classifications proposed for flood susceptibility using the HAND model

HAND (meters)	Classification
≤ 0	Inner-riverbeds (dry season) and water bodies
0 to 1	Major riverbeds (rainy season), flooded areas, swamps, and backswamps
1 to 5.5	Seasonally flooded areas due to annual extreme events
5.5 to 8	Areas with medium flood susceptibility in the case of inter-annual extreme events
8 to 10	Areas with low flood susceptibility in the case of inter-annual extreme events
10 to 15	Areas with very low flood susceptibility in the case of inter-annual extreme events
> 15	Areas without flood susceptibility

Source: the authors.

Table 5: Classifications proposed for flood susceptibility using the slope

Slope (%)	Classification
< 2%	Well-developed seasonal floodplains (provided that a floodplain is next to the river and the river is not entrenched)
2-5%	The possibility of flooding exists for small localized floodplains, and flood susceptibility exists in the case of extreme events
5-10%	Generally, no seasonal floodplains exist, but medium flood susceptibility exists in the case of extreme events
10-15%	Generally, no seasonal floodplains exist, but low flood susceptibility exists in the case of extreme events
> 15%	No flood susceptibility exists, except in the case of flash floods in areas that are very close to rivers

Source: the authors.

Table 6: Flood susceptibility classes combining HAND and slope indicators

Slope/HAND	< 1 m	1-5.5 m	5.5-8 m	8-10 m	10-15 m	> 15 m
< 2%	Very high	High	Medium	Low	Very low	No susceptibility
2-5%	High	Medium	Low	Very low	Very low	No susceptibility
5-10%	Medium	Low	Very low	Very low	Very low	No susceptibility
10-15%	Low	Very low	Very low	Very low	Very low	No susceptibility
> 15%	Very low	Very low	Very low	Very low	Very low	No susceptibility

Source: the authors.

There are many uses and concepts associated with the terms susceptibility, vulnerability and risk that are applied to flood contexts in the academic literature. In this

paper, we use the term susceptibility as an expression of the chance (frequency and associated uncertainty in temporal and spatial dimensions) of flood occurrence in each terrain pixel. The term susceptibility was chosen because part of the academic literature uses the term vulnerability as a combination of susceptibility and the resilience/adaptation capacity, while other studies use the term risk as a combination of susceptibility and potential economic-social-environmental losses (MERZ et al., 2007; BMZ; 2014).

The HAND indicator raster was truncated to integer values in ArcGIS 10.2 using the “Int” algorithm in the Spatial Analyst extension. Subsequently, the “Zonal Statistics as Table” algorithm was used to calculate the average value of the floodable cross-sectional area for each integer value of HAND. Then, equations were modeled to estimate the classification limits of the floodable cross-sectional areas based on the classification of the HAND model.

Flood susceptibility maps were developed based on the (A) HAND model, (B) floodable cross-sectional area, (C) conventional slope, (D) slope to the nearest drainage, (E) combination of HAND and the conventional slope, (F) combination of the floodable cross-sectional area and conventional slope, (G) combination of HAND and the slope to the nearest drainage, and (H) combination of the floodable cross-sectional area and slope to the nearest drainage. The choice of indicators in this paper combines the academic research line that uses the HAND model (Table 2) with the academic research line that uses slope conjugated with horizontal distance (Table 3). Figure 4 presents the general methodology of this paper.

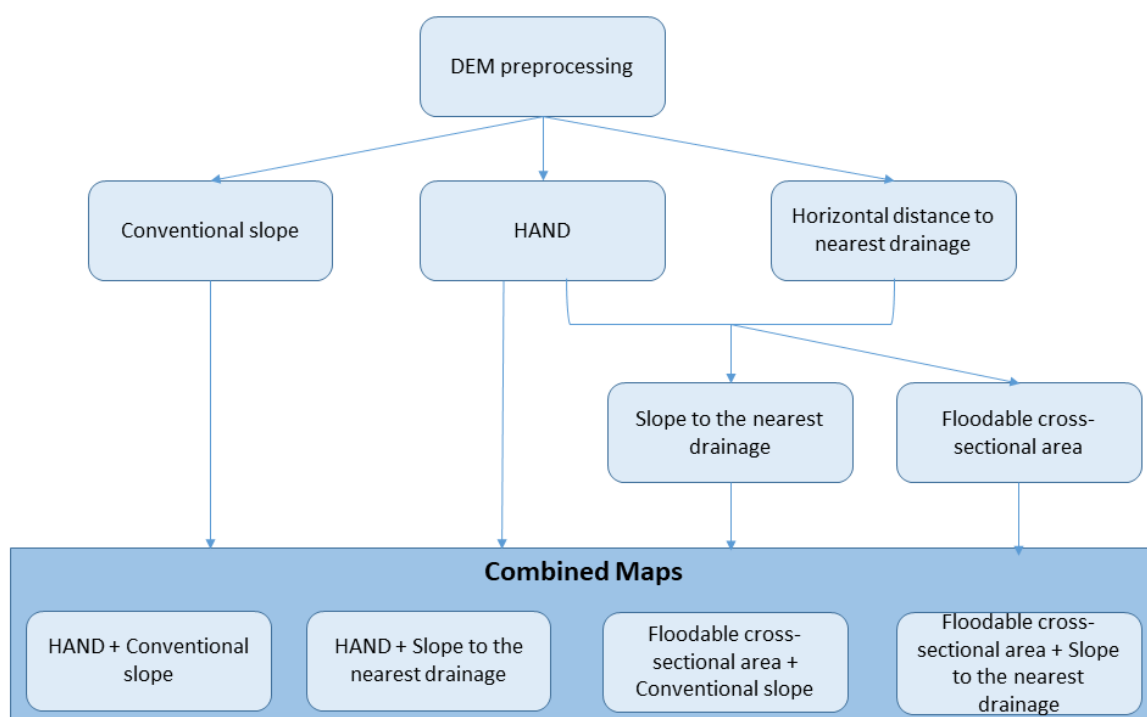


Figure 4: Methodology for flood susceptibility maps

Source: the authors.

RESULTS AND DISCUSSION

The results of each methodological step for the entire SRTM scene are available in the supplementary material at: <<https://app.box.com/s/bbbi951c7pqc8xyh6ukyhh11osz4lhc>>. The comparison between the HAND values from 0 to 35 and the average values of floodable cross-sectional area for the entire SRTM scene are plotted in Figure 5. Additionally, the graph shows a regression function that relates both variables.

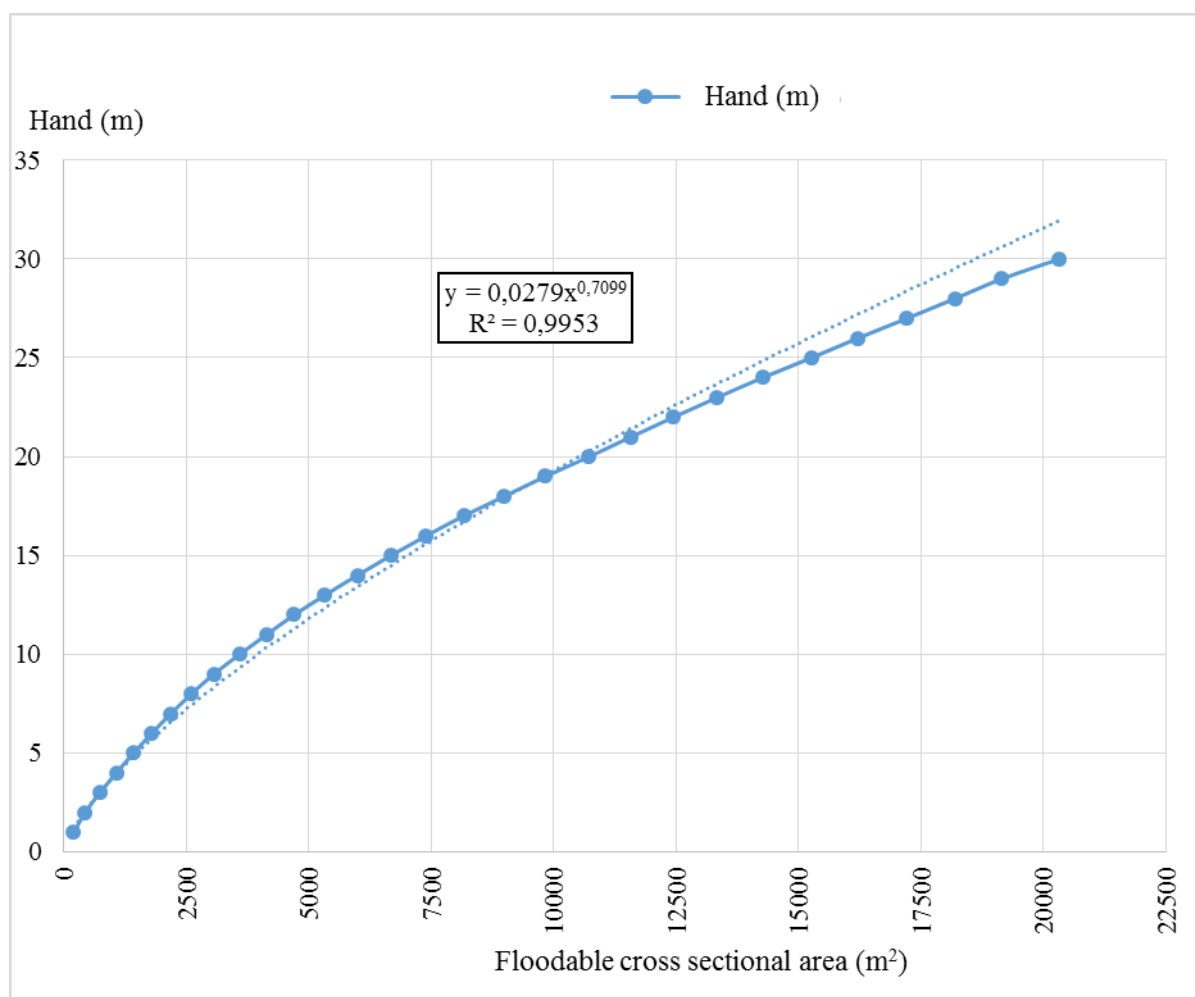


Figure 5: Graph comparing the mean values of the HAND indicator and the floodable cross-sectional area, as well as the regression between these two variables

Source: the authors.

Based on the relationship between HAND and floodable cross-sectional area presented in Figure 5, Table 7 replaces the values of HAND of Table 4 with the respective values of the floodable cross-sectional area. Analogously, Table 8 replaces the HAND values of Table 6 with the respective values of the floodable cross-sectional area (from Figure 5), combined with the slope.

Table 7: Proposed classification for flood susceptibility based on the floodable cross-sectional area

Floodable cross-sectional area (m ²)	Classification
≤ 0	Inner-riverbeds (dry season) and water bodies
1 to 204	Major riverbeds (rainy season), flooded areas, swamps, and backwater areas
204 to 1606	Seasonally flooded areas due to annual extreme events
1606 to 2605	Areas with medium flood susceptibility in the case of inter-annual extreme events
2605 to 3589	Areas with low flood susceptibility in the case of inter-annual extreme events
3589 to 6681	Areas with very low flood susceptibility in the case of inter-annual extreme events
> 6681	Areas without flood susceptibility

Source: the authors.

Table 8: Flood susceptibility classes combining the HAND and slope indicators

Slope (%)/Floodable cross-sectional area (m ²)	< 204	204-1606	1606-2605	2605-3589	3589-6681	> 6681
< 2%	Very high	High	Medium	Low	Very low	No susceptibility
2-5%	High	Medium	Low	Very low	Very low	No susceptibility
5-10%	Medium	Low	Very low	Very low	Very low	No susceptibility
10-15%	Low	Very low	Very low	Very low	Very low	No susceptibility
> 15%	Very low	Very low	Very low	Very low	Very low	No susceptibility

Source: the authors.

Figures 6 and 7 present maps of flood susceptibility based on HAND and the floodable cross-sectional area, using the classes proposed in Tables 4 and 7. The area visualized is interesting in terms of its fluvial geomorphological diversity. In the northwest, there are springs on a higher plateau. In the southwest, there are entrenched river valleys running through a hilly relief. In the center, there is a river with a wide floodplain. In the east, there is another river with an entrenched valley on a plateau.

Figures 6 and 7 are similar, especially because the cross-sectional area classes were calibrated based on HAND classes. However, some areas with low HAND values located relatively far from rivers exhibited low susceptibility in the map based on the cross-sectional area, especially near the springs of the northwestern plateau. On the other hand, the map of cross-sectional area expanded regions of flood susceptibility near rivers with entrenched valleys.

Figures 8 and 9 illustrate maps of the susceptibility classes based only on the conventional slope and the slope to the nearest drainage using the classes proposed in Table 5. Plain areas (slopes of up to 2%), including floodplains and hilltops, dominate the region. Areas with gentle slopes (2 to 5%) can be observed on hillslopes that separate floodplains and hilltops. Areas with slopes greater than 5% are restricted the borders of plateaus in the

conventional slope map (Figure 8) and to entrenched river valleys in the slope to the nearest drainage map (Figure 9). This suggests that despite the relevant influence of the slope on flood susceptibility in this region, an analysis based on the slope alone cannot differentiate between high-susceptibility floodplain areas and low-susceptibility hilltop areas.

A comparison of the conventional slope map (Figure 8) with the map of slope to the nearest drainage (Figure 9) shows good agreement between high slope classes (2 to 5%) near watercourses in entrenched valleys. However, in pixels far from rivers, the horizontal component of slope to the nearest drainage dominates; therefore, the classes tend to low values. In areas with local ruggedness that are near watercourses and relatively low in relation to the drainage, the slope to the nearest drainage yields lower values than the conventional slope. However, on the tops of terraces near rivers, even when the conventional slope is low, the slope to the nearest drainage yields higher values due to the reference of these values to streams.

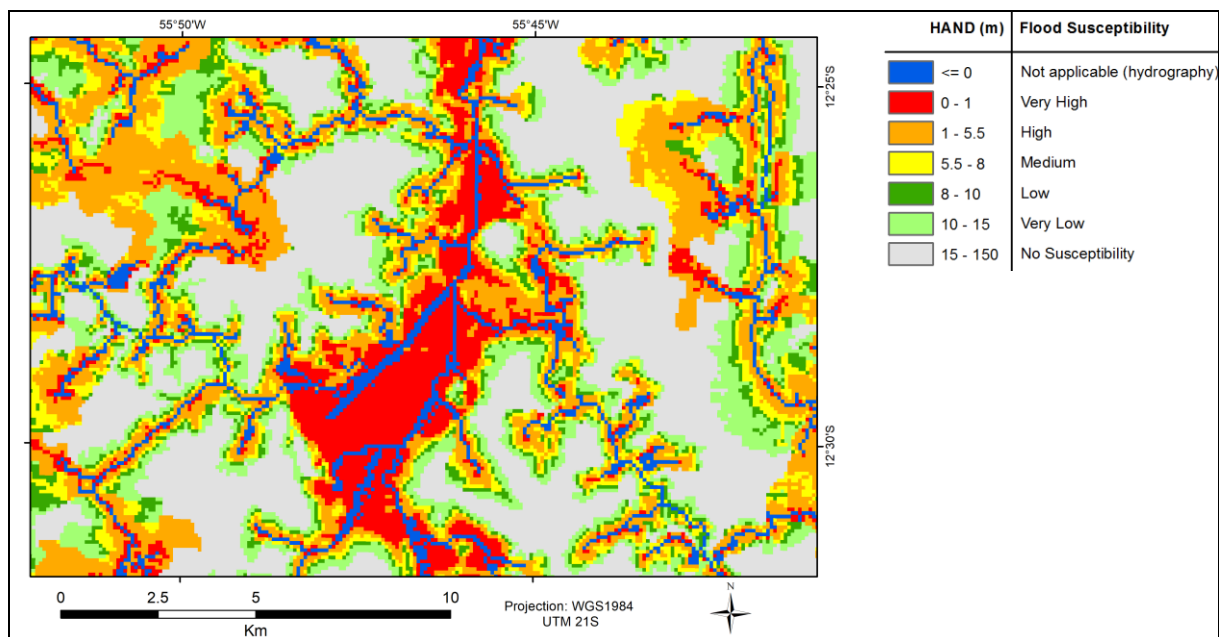


Figure 6: Flood susceptibility according to the HAND indicator

Source: the authors.

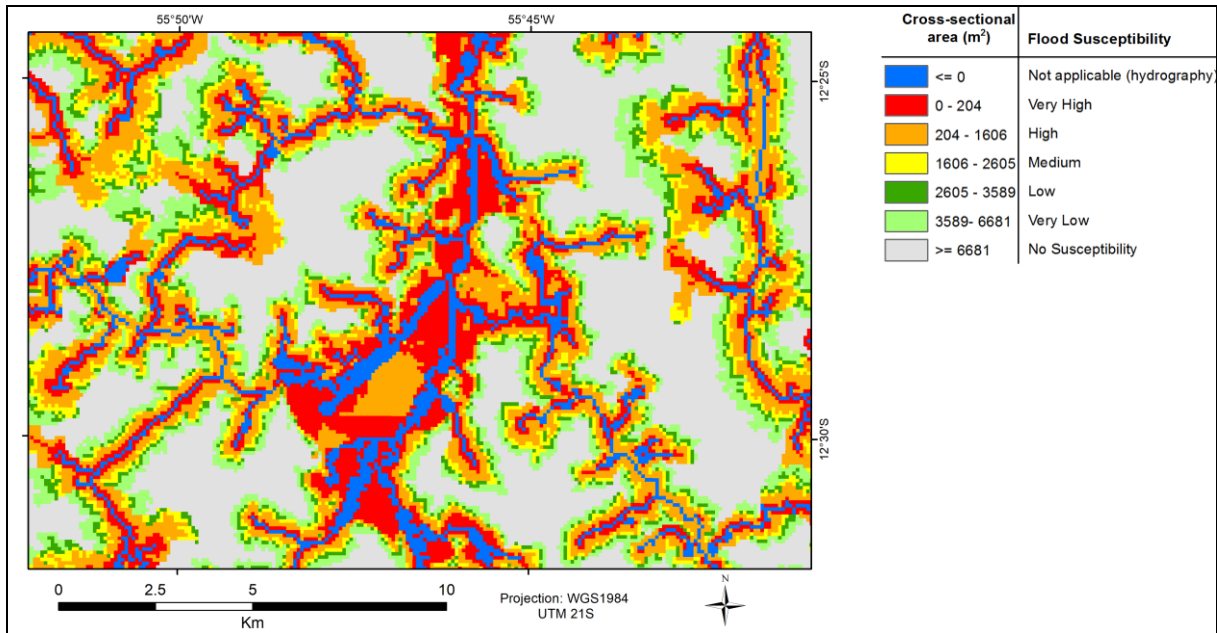


Figure 7: Flood susceptibility according to the floodable cross-sectional area
Source: the authors.

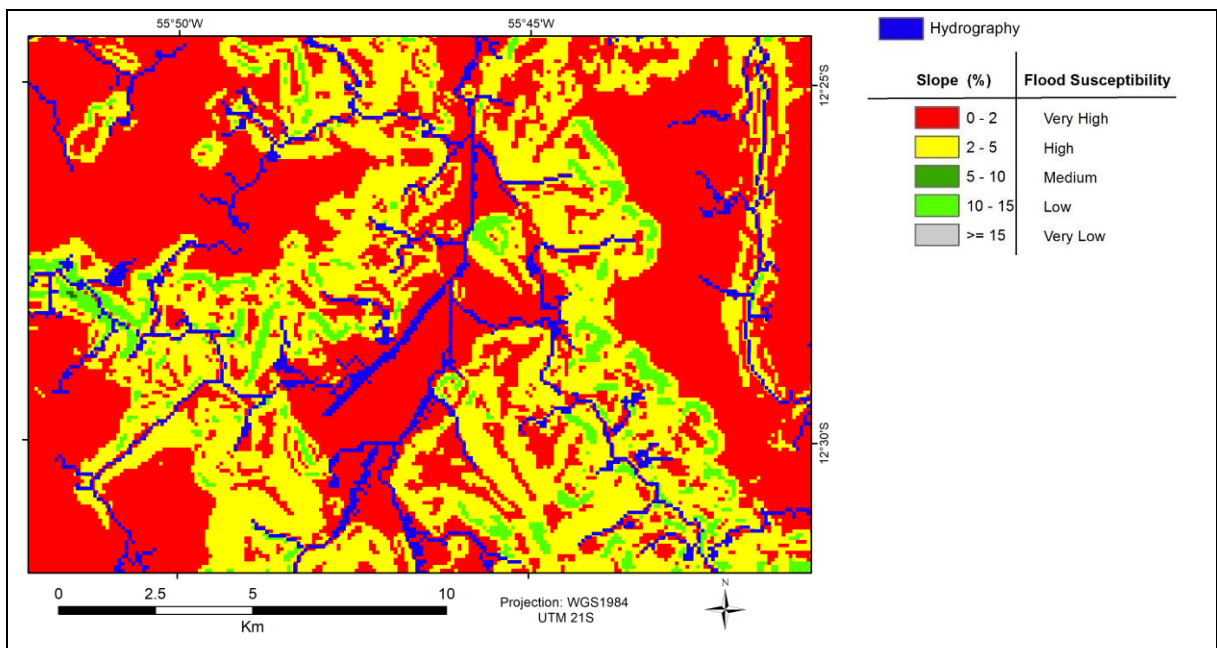


Figure 8: Flood susceptibility according to the conventional slope
Source: the authors.

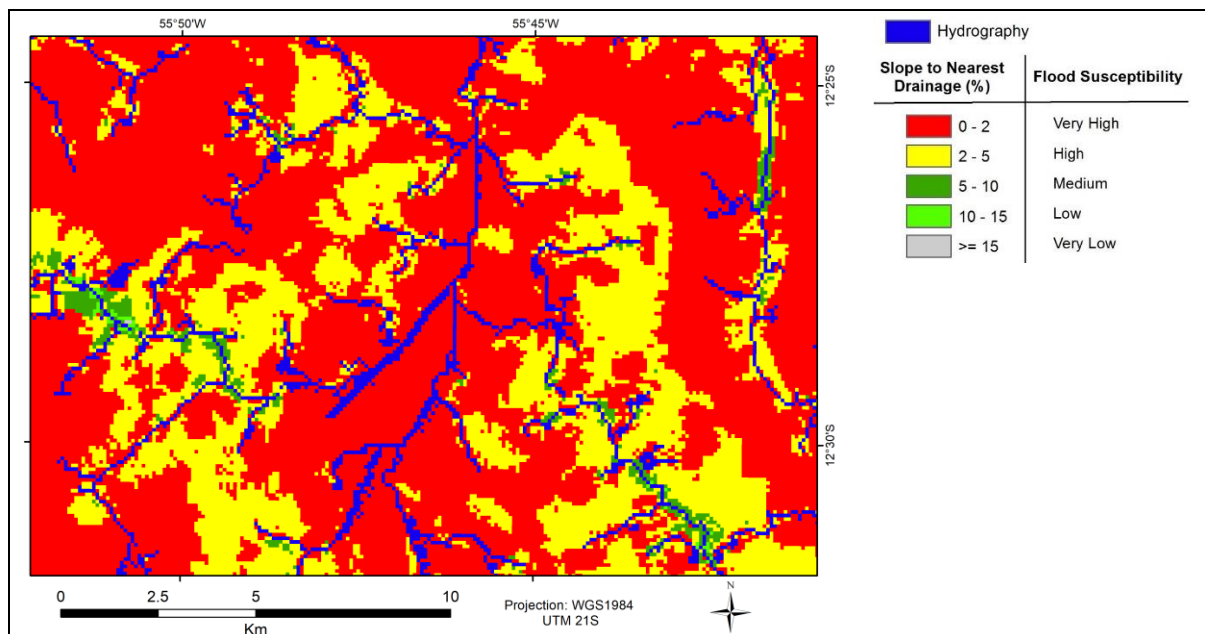


Figure 9: Flood susceptibility according to the slope to the nearest drainage

Source: the authors.

Figures 10 and 11 show the flood susceptibility maps based on HAND, the conventional slope and slope to the nearest drainage, for the classification values proposed in Table 6. Figure 12 shows a flood susceptibility map based on the floodable cross-sectional area and the conventional slope for the values proposed in Table 8. Figure 13 presents a map that combines cross-sectional area with the slope to the nearest drainage. In the four maps (Figures 10 to 13), the slope helped restrict areas of high and very high susceptibility to regions within flood plains. In addition, the slope decreased the susceptibility near the borders of plains due to hillslope breaks. For rivers in entrenched valleys, the slope generally reduced the flood susceptibility even more.

In general, the maps that used the conventional slope as auxiliary information (Figures 10 and 12) are very similar to the ones that used the slope to the nearest drainage (Figures 11 and 13). However, a detailed inspection suggests that susceptibility increased in some rugged areas next to rivers because the slope to the nearest drainage was lower than the conventional slope. These are areas with micro-ruggedness that are still close to the water level. In contrast, the flood susceptibility decreased more in small plain areas on the tops of terraces next to rivers in the maps that conjugated slope to the nearest drainage because its values were higher than those calculated using the conventional slope.

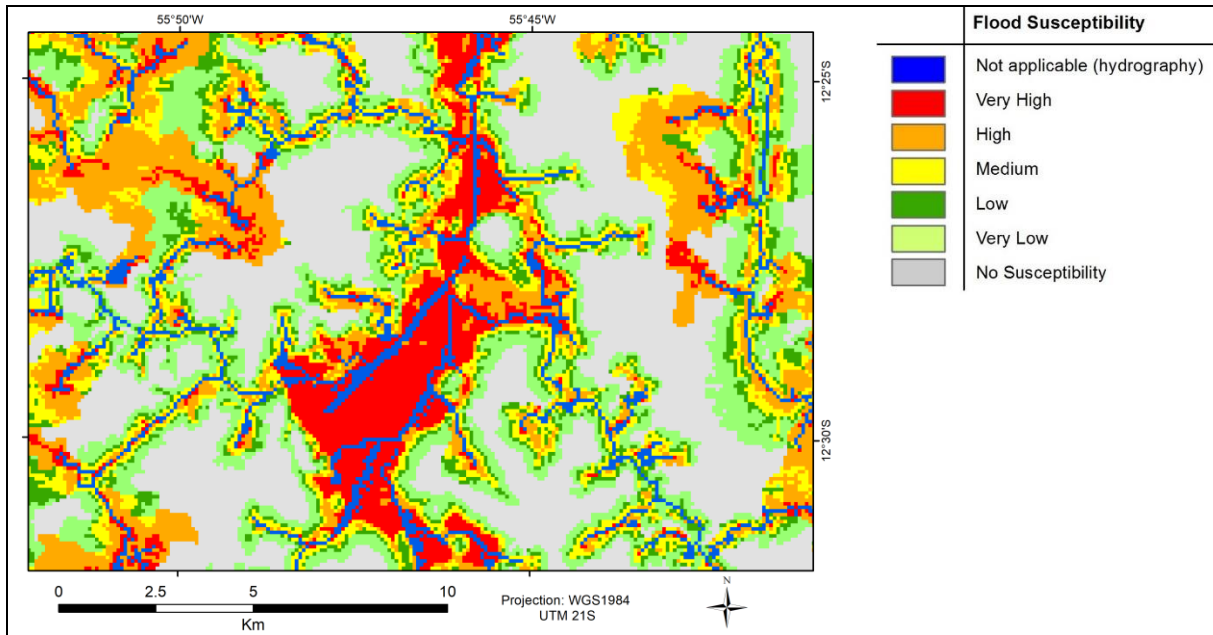


Figure 10: Flood susceptibility according to the combination of HAND and the conventional slope

Source: the authors.

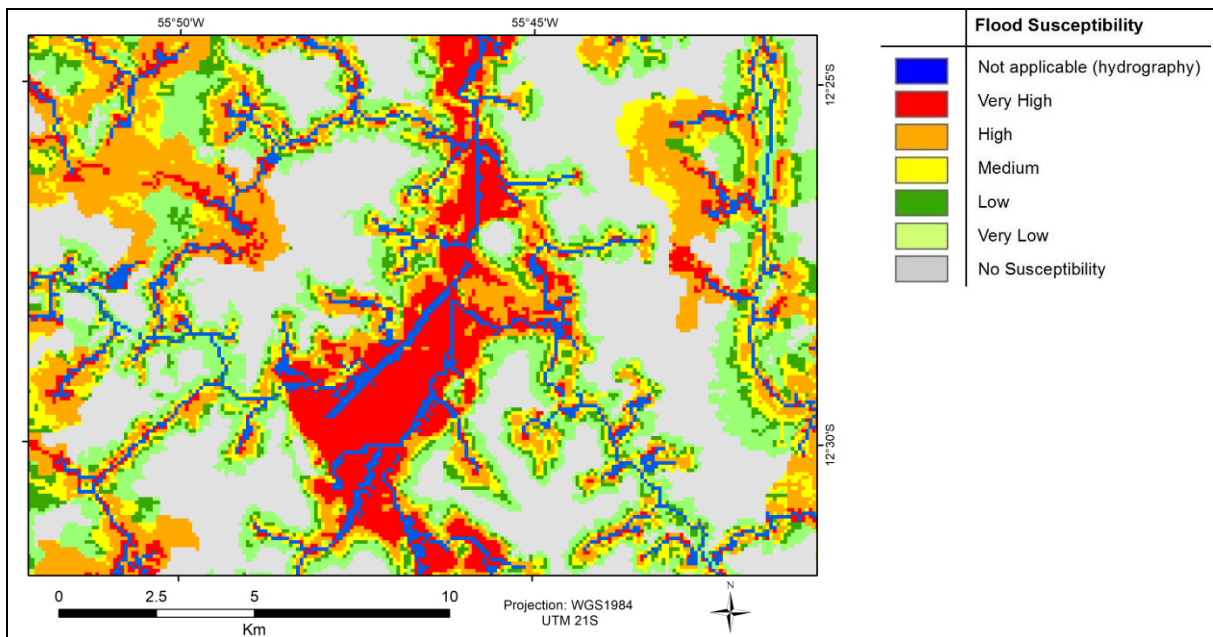


Figure 11: Flood susceptibility according to the combination of HAND and the slope to the nearest drainage

Source: the authors.

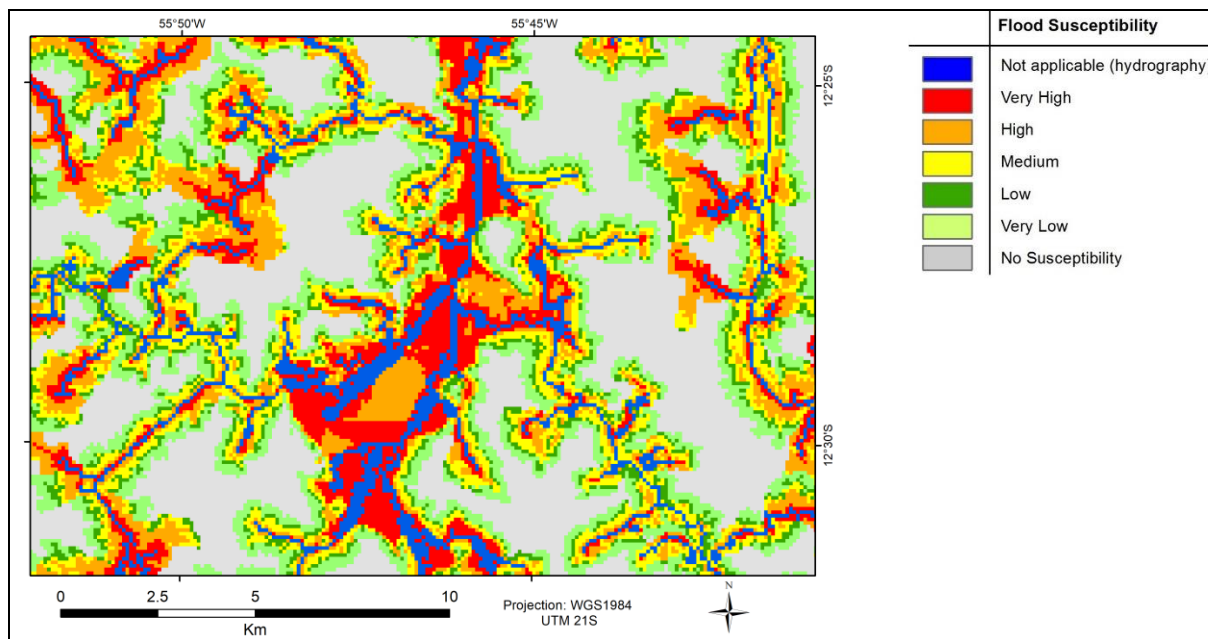


Figure 12: Flood susceptibility according to the combination of the floodable cross-sectional area and conventional slope
Source: the authors.

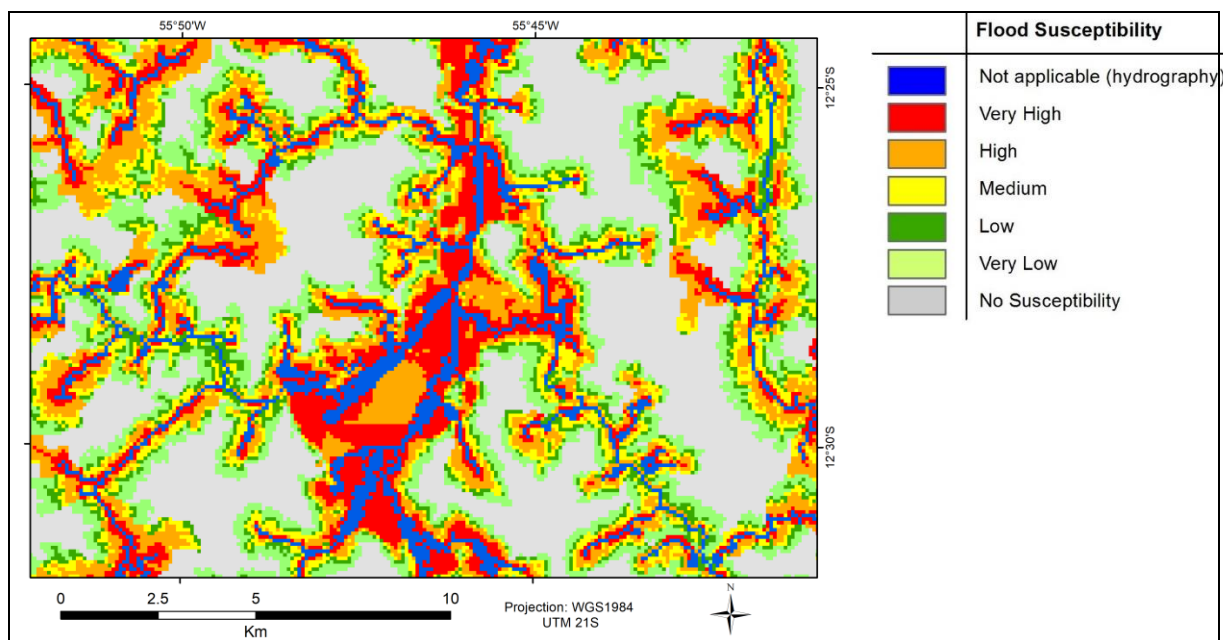


Figure 13: Flood susceptibility according to the combination of the floodable cross-sectional area and the slope to the nearest drainage
Source: the authors.

One limitation of the approaches based on the floodable cross-sectional area and slope to the nearest drainage is that if one side of the river margin is lower than the opposite side, the water will tend to flood more on the lower side. Hydraulic models could better evaluate this type of flooding process. Moreover, the two indicators assume that a terrain cross-section

is an inclined plain without curvature, and a more concave or convex valley would yield less accurate results for both indicators (Figure 14).

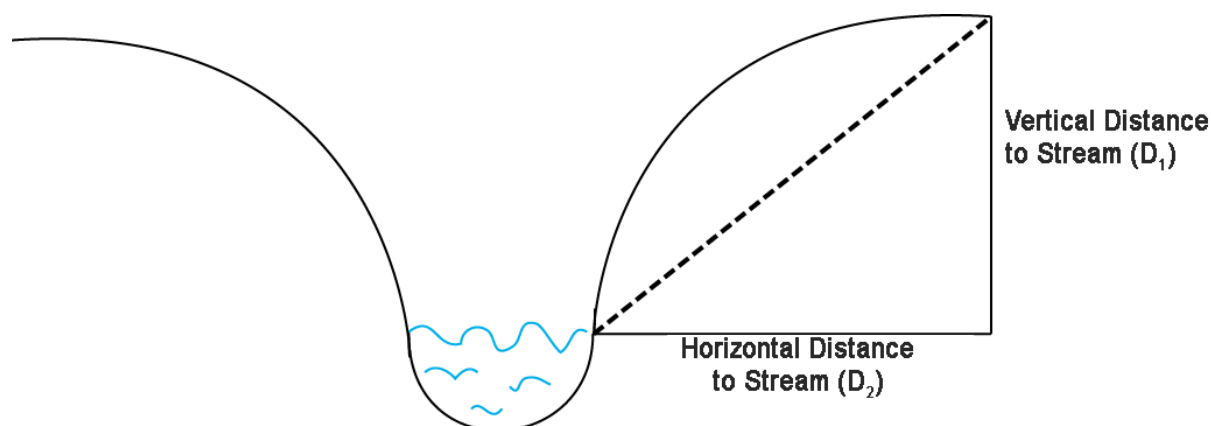


Figure 14: Hypothetical case of the imprecision of the floodable cross-sectional area and slope to the nearest drainage indicators in valleys with convex relief

Source: the authors.

CONCLUSIONS

The resources (digital elevation models and hydrography) and methodological procedures (software and algorithms) used in this paper were appropriate for the analysis in the spatial context of this research, in relation to its analyzed scale/reality; i.e., they were satisfactory for the proposed analysis and did not need any adaptation. This indicates that the tools for the HAND model (Table 1) have developed and matured enough in past years to be applied to studies of this nature, as has been already demonstrated by the large body of academic literature (Table 2).

The use of slope as a complementary indicator contributed to containing the flood susceptibility classification to the fluvial plains. Both the slope to the nearest drainage and the floodable cross-sectional area exhibited spatial patterns that were consistent with the expected underlying hydrological processes. The indicator of floodable cross-sectional area, especially when combined with slope, resulted in a more spatially restricted susceptibility than when compared to the HAND model.

However, despite using classification schemes for HAND and slope based on the academic literature, it is necessary to acknowledge that this paper lacks empirical validation from ground truth or remote sensing data, and such data are necessary to evaluate the efficiency of the resulting maps. Nevertheless, the multiple combinations of indicators helped to illustrate the spatial behaviors and consistencies of each proposed indicator regarding the

plausible hydrological and environmental characteristics (Tables 4, 5 and 7) of the study area. Future studies based on hydrological data, civil defense databases and Sentinel radar images could be conducted to validate the proposed methodology. Additionally, further studies could determine the indicators and maps that are more accurate for analyses of flash floods or slow floodplain overflow, and other studies could validate the classification schemes (HAND, floodable cross-sectional area, conventional slope, and slope to the nearest drainage) in distinct geomorphological and anthropogenic-based contexts (impervious land, dams, canal construction, etc.).

ACKNOWLEDGMENTS

We thank FAPEMIG (Tecnova Edital, 13/2013), CNPq (MCTI/SETEC/CNPq Edital n. 54/2013, RHAE) and FINEP for supporting this research. Additionally, we thank WayCarbon for the development and support of the Model for Vulnerability Evaluation (MOVE), which includes the methods presented in this paper.

REFERENCES

ALFAYA, F. A. V. S. **Mapeamento de áreas alagáveis da calha Solimões/Amazonas utilizando análise de imagens baseada em objeto com dados MDE-SRTM**. 2012. 59 f. Dissertação (Mestrado em Sensoriamento Remoto) – INPE, São José dos Campos - SP, 2012. Disponível em: <<http://mtc-m16d.sid.inpe.br/col/sid.inpe.br/mtc-m19/2012/04.10.11.22/doc/publicacao.pdf>>. Acesso em: 09 maio 2017.

BMZ. Federal Ministry for Economic Cooperation and Development. **The vulnerability Sourcebook** – concept and guidelines for standardized vulnerability assessment. Germany: GIZ, Adelphi and EURAC, 2014.

CHAVES, I. S. B.; PEIXOTO FILHO, G. E. Identificação de áreas suscetíveis à ocorrência de inundações na Região Administrativa Fercal (RA XXXI). SIMPÓSIO BRASILEIRO DE SENSORIAMENTO REMOTO – SBSR, 17., 2015, João Pessoa. **Anais eletrônicos...** João Pessoa-PB: INPE, 2015. Disponível em: <<http://www.dsr.inpe.br/sbsr2015/files/p1546.pdf>>. Acesso em: 19 fev. 2017.

COOPER, V.; OPADEYI J. **Flood Hazard Mapping of St. Lucia**. Caribbean Development Bank, 2006. 31p. Disponível em: <[http://www.researchgate.net/publications.PublicPostFileLoader.html?id=51abca3ed3df3e257b000065&key=5046351abca3ed16e2](http://www.researchgate.net/publications/PublicPostFileLoader.html?id=51abca3ed3df3e257b000065&key=5046351abca3ed16e2)>. Acesso em: 19 fev. 2017.

DED, M. Hydrogeomorphological Method of Floodplain Delineation. **Geographia Technica**, v. 8, n. 2, p. 13-22, 2013. Disponível em: <http://technicalgeography.org/pdf/2_2013/02_ded.pdf>. Acesso em: 19 fev. 2017.

DIAS, A. P. **Análise espacial aplicada à delimitação de áreas úmidas da planície de inundação do médio Araguaia**. 2014. 91 f. Dissertação (Mestrado em Ciências Florestais e Ambientais) – Universidade Federal de Mato Grosso, Cuiabá-MT, 2014. Disponível em: <<http://www.ufmt.br/ufmt/unidade/userfiles/publicacoes/99d8c652da761d3c30f7a3e39d05e8f5.pdf>>. Acesso em: 19 fev. 2017.

GAO, H.; HRACHOWITZ, M.; FENICIA, F. F.; GHARARI, S.; SAVENIJE, H. H. G. Testing the realism of a topography-driven model (FLEX-Topo) in the nested catchments of the Upper Heihe, China. **Hydrology and Earth System Sciences**, n. 18, 2014. Disponível em: <<http://www.hydrol-earth-syst-sci.net/18/1895/2014/hess-18-1895-2014.html>>. Acesso em: 19 fev. 2017.

GHARARI, S.; HRACHOWITZ, M.; FENICIA, F.; SAVENIJE, H. H. G. Hydrological landscape classification: investigating the performance of HAND based landscape classifications in a central European meso-scale catchment. **Hydrology and Earth System Sciences**, v. 15, n. 11, p. 3275-3291, 03 nov. 2011a. Disponível em: <<http://doi.org/10.5194/hess-15-3275-2011>>. Acesso em: 19 fev. 2017.

GHARARI, S.; FENICIA, F.; SAVENIJE, H. Hydrological Land Classification Based on Landscape Units. **AGU Fall Meeting Abstracts**, v. 1, 2011b.

GHARARI, S.; HRACHOWITZ, M.; FENICIA, F.; GAO, H.; SAVENIJE, H. H. G. Using expert knowledge to increase realism in environmental system models can dramatically reduce the need for calibration. **Hydrology and Earth System Sciences**, v. 18, n. 12, p. 4839-4859, 2014.

GUZINSKI, R.; KASS, S.; HUBER, S.; BAUER-GOTTWEIN, P.; JENSEN, I.H.; NAEIMI, V.; DOUBKOVA, M.; WALLI, A.; TOTTRUP, C. Enabling the Use of Earth Observation Data for Integrated Water Resource Management in Africa with the Water Observation and Information System. **Remote Sensing**, v. 6, n. 8, p. 7819-7839, 2014. Disponível em: <<https://www.mdpi.com/2072-4292/6/8/7819/pdf>>. Acesso em: 19 fev. 2017.

JARVIS, A.; REUTER, H. I.; NELSON, A.; GUEVARA, E. **Hole-filled SRTM for the globe Version 4**. CGIAR-SXI SRTM 90m database. 2008. Disponível em: <<http://srtm.csi.cgiar.org>>. Acesso em: 31 mar. 2013.

MENGUE, V. P. **Avaliação da dinâmica espectro-temporal visando o mapeamento da soja e arroz irrigado no Rio Grande do Sul**. 2013. 122 f. Dissertação (Mestrado em Sensoriamento Remoto) – Centro Estadual de Pesquisas em Sensoriamento Remoto e Meteorologia, Universidade Federal do Rio Grande do Sul, Porto Alegre, 2013. Disponível em: <<http://repositorio.ufrgs.br/handle/10163/10000>>. Acesso em: 19 fev. 2017.

em: <<https://www.lume.ufrgs.br/bitstream/handle/10183/87991/000912244.pdf?sequence=1>>. Acesso em: 19 fev. 2017.

MERZ, B.; THIEKEN, A. H.; GOCHT, M. Flood risk mapping at the local scale: concepts and challenges. In: BEGUM, S.; STIVE, M. J. F.; HALL, J. W. (Ed.). **Flood risk management in Europe: innovation in policy and practice**. USA: Springer Netherlands, 2007. p. 231-251.

MESA, G. J. P. **Propuesta metodológica para la estimación de zonas de inundación con información escasa por medio de descriptores geomorfométricos derivados de modelos digitales de elevación**. Tesis (Maestría en Ingeniería – Recursos Hidráulicos) – Universidad Nacional de Colombia, Medellín, 2014. Disponível em: <<http://www.bdigital.unal.edu.co/44831/1/1037603675.2014.pdf>>. Acesso em: 19 fev. 2017.

MOREIRA, C. V. R.; PIRES NETO, A. G. Clima e Relevo. In: OLIVEIRA, A. M. S.; BRITO, S. N. A. **Geologia da Engenharia**. São Paulo: Associação Brasileira de Geologia de Engenharia, 1998. p. 69-85.

NOBRE, C. A.; YOUNG, A. F.; SALDIVA, P. H. N.; ORSINI, J. A. M.; NOBRE, A. D.; AGURA, A. T.; THOMAZ, O. PÁRRAGA, G. O. O.; SILVA, G. C. M.; VALVERDE, M.; SILVEIRA, A. C.; RODRIGUES, G. O. Vulnerability of Brazilian Megacities to climate change: the São Paulo Metropolitan region (RMSP). In: MOTTA, R. S.; HARGRAVE, J.; LUEDEMANN, G.; GUTIERREZ, M. B. S. (Ed.). **Climate Change in Brazil: economic, social and regulatory aspects**. Brasília: IPEA, 2011a, 197 p. Disponível em: <<http://citeseerx.ist.psu.edu/viewdoc/download?doi=10.1.1.470.2080&rep=rep1&type=pdf#page=198>>. Acesso em: 19 fev. 2017.

NOBRE, A. D.; CUARTAS, L. A.; HODNETT, M.; RENNÓ, C. D.; RODRIGUES, G.; SILVEIRA, A.; WATERLOO, M.; SALESKA, S. Height Above the Nearest Drainage – a hydrologically relevant new terrain model. **Journal of Hydrology**, v. 404, n. 1, p. 13-29, 2011b.

NOBRE, A. D.; CUARTAS, L. A.; MOMO, M. R.; SEVERO, D. L.; PINHEIRO, A.; NOBRE, C. A. HAND contour: A new proxy predictor of inundation extent. **Hydrological Processes**, v. 30, n. 2, p. 320-333, 2016. Disponível em: <<http://onlinelibrary.wiley.com/doi/10.1002/hyp.10581/full>>. Acesso em: 19 fev. 2017.

NSW Department of Natural Resources. Carroona-Breeza Floodplain Management Plan. 2006. Disponível em: <<http://www.environment.nsw.gov.au/resources/floodplains/CarroonaBreezaFMP.pdf>>. Acesso em: 19 fev. 2017.

PRINA, Z. B.; TRETIN, R. Metodologia para mapeamento de áreas suscetíveis à inundação: estudo de caso para o município de Jaguari – RS. CONGRESSO BRASILEIRO DE

CARTOGRAFIA, 26., 2014, Gramado. **Anais eletrônicos...** Gramado, RS: CBC, 2014, n.274. Disponível em: <http://www.cartografia.org.br/cbc/trabalhos/1/274/CT01-9_1403562395.pdf>. Acesso em: 19 fev. 2017.

RENNÓ, C. D.; NOBRE, A. D.; CUARTAS, L. A.; SOARES, J. V.; HODNETT, M. G.; TOMASELLA, J.; WATERLOO, M. J. HAND, a new terrain descriptor using SRTM-DEM: Mapping terra-firme rainforest environments in Amazonia. **Remote Sensing of Environment**, v. 112, n. 9, p. 3469-3481, 2008. Disponível em: <<http://www.sciencedirect.com/science/article/pii/S0022169411002599>>. Acesso em: 19 fev. 2017.

RODRIGUES, G. O.; NOBRE, A. D.; SILVEIRA, A. C.; CUARTAS, L. A. Efeitos da resolução espacial de dados SRTM na descrição de terrenos obtida pelo modelo HAND (Height Above the Nearest Drainage) – estudo de caso em Manaus/AM. SIMPÓSIO BRASILEIRO DE SENSORIAMENTO REMOTO - SBSR, 15., 2011, Curitiba. **Anais eletrônicos...** Curitiba: INPE, 2011. p. 5769. Disponível em: <<http://www.dsr.inpe.br/sbsr2011/files/p1379.pdf>>. Acesso em: 19 fev. 2017.

ROSGEN, D. L. A classification of natural rivers. **Catena**, v. 22, n. 3, p. 169-199, 1994. Disponível em: <<http://pages.geo.wvu.edu/~kite/Rosgen1994ClassificationRivers.pdf>>. Acesso em: 19 fev. 2017.

SANTOS, E.M.; SOBREIRA, F.G.; BARELLA, C.F. Mapeamento de áreas susceptíveis a inundação a partir do modelo Hand. SEIC, 21., 2013, Ouro Preto. **Anais eletrônicos...** Ouro Preto: UFOP, 2013. Disponível em: <<http://www.portalpet.feis.unesp.br/media/grupos/pet-sistemadeinformacao-seropedica/atividades/xiv-sudeste-pet-rj-2014/artigos/Eugenia.doc>>. Acesso em: 19 fev. 2017.

SCHLAFFER, S.; HOLLAUS, M.; WAGNER, W.; MATGEN, P. Flood delineation from synthetic aperture radar data with the help of a priori knowledge from historical acquisitions and digital elevation models in support of near-real-time flood mapping. In: **SPIE Remote Sensing**, International Society for Optics and Photonics, p. 853813-853813, october 2012. Disponível em: <<https://doi.org/10.1117/12.974503>>. Acesso em: 19 fev. 2017.

SCHLAFFER, S.; MATGEN, P.; HOLLAUS, M.; WAGNER, W. Flood detection from multi-temporal SAR data using harmonic analysis and change detection. **International Journal of Applied Earth Observation and Geoinformation**, v. 38, p. 15-24, 2015. Disponível em: <<http://www.sciencedirect.com/science/article/pii/S0303243414002645>>. Acesso em: 19 fev. 2017.

SILVA, J. A. A.; NOBRE, A. D.; MANZATTO, C. V.; JOLY, C. A.; RODRIGUES, R. R.; SKORUPA, L. A.; NOBRE, C. A.; AHRENS, S.; MAY, P. H.; SÁ, T. D. A.; CUNHA, M. C.; RECH FILHO, E. L. **O Código Florestal e a Ciência**: contribuições para o diálogo. São Paulo: SBPC, 2011.

SILVA, W. F.; MOLLERI, G. S. F.; PINTO, M. B. P. Análise do modelo HAND para a indicação de áreas suscetíveis a eventos críticos de cheias. In: SIMPÓSIO BRASILEIRO DE SENSORIAMENTO REMOTO - SBSR, 16., 2013, Foz do Iguaçu. **Anais eletrônicos...** Foz do Iguaçu, PR: INPE, 2013. Disponível em: <<http://www.dsr.inpe.br/sbsr2013/files/p0693.pdf>>. Acesso em: 19 fev. 2017.

TEMPORIM, F. A.; ALVARENGA, C. A. T.; FORTES, P. T. F. O. Estudo de manchas de inundação utilizando imagem SRTM nas proximidades da área urbanizada da sede do município de Alegre-ES. In: SIMPÓSIO BRASILEIRO DE SENSORIAMENTO REMOTO - SBSR, 16., 2013, Foz do Iguaçu. **Anais eletrônicos...** Foz do Iguaçu, PR: INPE, 2013. Disponível em: <<http://www.dsr.inpe.br/sbsr2013/files/p1093.pdf>>. Acesso em: 19 fev. 2017.

TRENTIN, R.; ROBAINA, L. E. S. Análise do relevo no alto curso da bacia hidrográfica do Rio Itu, RS. **Interface**, Porto Nacional/TO, v. 2, n. 2. p. 146-155, maio 2005. Disponível em: <<http://revista.uft.edu.br/index.php/interface/article/viewFile/339/236>>. Acesso em: 19 fev. 2017.

VARALLO, L.; PRETE, V. D.; FALCAO, K.; MOMM-SCHULT, S. I.; TRAVASSOS, L.; CANIL, K. Metodologia para elaboração da Carta de Aptidão à Urbanização: mapeamento e propostas para áreas úmidas em São Bernardo do Campo. In: CONGRESSO DA SOCIEDADE DE ANÁLISE DE RISCO LATINO AMERICANA, 3., 2016, São Paulo. **Anais...** São Paulo: ABGE, 2016.

ZEVENBERGEN, L. W.; THORNE, C. R. Quantitative analysis of land surface topography. **Earth Surface Processes and Landforms**, v. 12, p. 47-56, 1987.

WESTERHOFF, R. S.; KLEUSKENS, M. P. H.; WINSEMIUS, H. C.; HUIZINGA, H. J.; BRAKENRIDGE, G. R.; BISHOP, C. Automated global water mapping based on wide-swath orbital synthetic-aperture radar. **Hydrology and Earth System Sciences**, v. 17, n. 2, p. 651-663, fev. 2013. Disponível em: <<http://doi.org/10.5194/hess-17-651-2013>>. Acesso em: 19 fev. 2017.